# Update on studies of the FDC prototype and test stand setup

Simon Taylor and Daniel S. Carman
Ohio University

August 19, 2005

**Abstract**

We present an update on recent advances in the prototype studies underway in the Test Lab. The quality of the tracking using the test stand chambers has improved to the point that we have started to use this data to study the performance of the prototype. We also report some preliminary studies using a Struck Flash-ADC.

Some significant advances in the hardware in the Test Lab area and in our understanding of the performance of the prototype have been made since the previous hardware report[1]. We have replaced the FASTBUS crate with a VME-64x crate. We are using two CAEN V792 ADCs to read out the analog signals from the strips and an F1 TDC to digitize the signals from the test stand chambers. We found and fixed an error in the construction of the anode wire plane of the prototype (some resistors were left off, causing all the wires to be OR'ed together). This plane does not contain any field wires. The trigger, gas mixture, and configuration of the cathode planes are the same as before.

In the previous report[1] only information from the prototype itself was needed to give us some idea of the resolution of the device. In order to gain some understanding of the performance of the prototype for the x-coordinate (away from the wire), we need well-reconstructed tracks through the test stand chamber stacks, which in turn requires a time-to-distance calibration for each of the layers in the two stacks. A sample drift time distribution for one of the four layers in the x-stack and its integral is shown in figure 1. The

maximum drift time $t_{max}$ is determined from a fit to the falling edge of the distribution. The functional form is [2]

$$F(t) = p_m + \frac{a_m t + A_m}{1 + \exp\left(\frac{t - t_m}{T_m}\right)}, \tag{1}$$

$$t_{max} = t_m + T_m. \tag{2}$$

The black curve in the figure is the result of the fit. The right plot is the distribution of the integral of the left plot as a function of drift time. The ordinate is normalized to the integral between $t_0 = 0$ and $t_{max}$. The drift relation is determined via a sixth–order polynomial fit; this function must be multiplied by the cell size to obtain the time-to-distance calibration. The 15 cells in each chamber in the x- and y-stacks are assumed to behave the same so that there are only four such functions for the test stand chambers. Before these calibrations can be used to obtain good fits of muon tracks, the relative offsets in position between chambers need to be taken into account. Small offsets on the order of 1–2 mm in position (relative to our initial measurements of the test stand geometry) from cell to cell and offsets corresponding to a minimum drift distance (arising from the geometry of the test stand chambers) were needed to obtain the results shown in figure 2 for the x-stack; the results for the y-stack look the same and are not shown here. Only those events that have a single hit in each of the four layers of a given stack are used in the analysis. Since the muon tracks can pass on either side of a wire (this is the so-called "left-right ambiguity") in practice the fits are done multiple times either adding or subtracting the drift distance for each wire position and choosing the combination that gives the smallest $\chi^2$. The "residuals" are the differences between the projection from the track fit to the position at a given plane and the measurement (after the left-right ambiguity has been resolved). Gaussian fits to the residuals for each layer in the x-stack are shown in figure 3. The resolution for both stacks as tabulated in Table 1 is on the order of 220 $\mu$m at each of the test stand planes, which is good enough for a meaningful study of the prototype resolution using tracks through the test stand.

The y-position[1] at the plane of the prototype wires of a muon track passing through the prototype is determined by combining the strip information from both views (above and below the wire plane). The procedure

[1]Since the avalanche occurs very close to the wire, the x coordinate is quantized by the wire position.

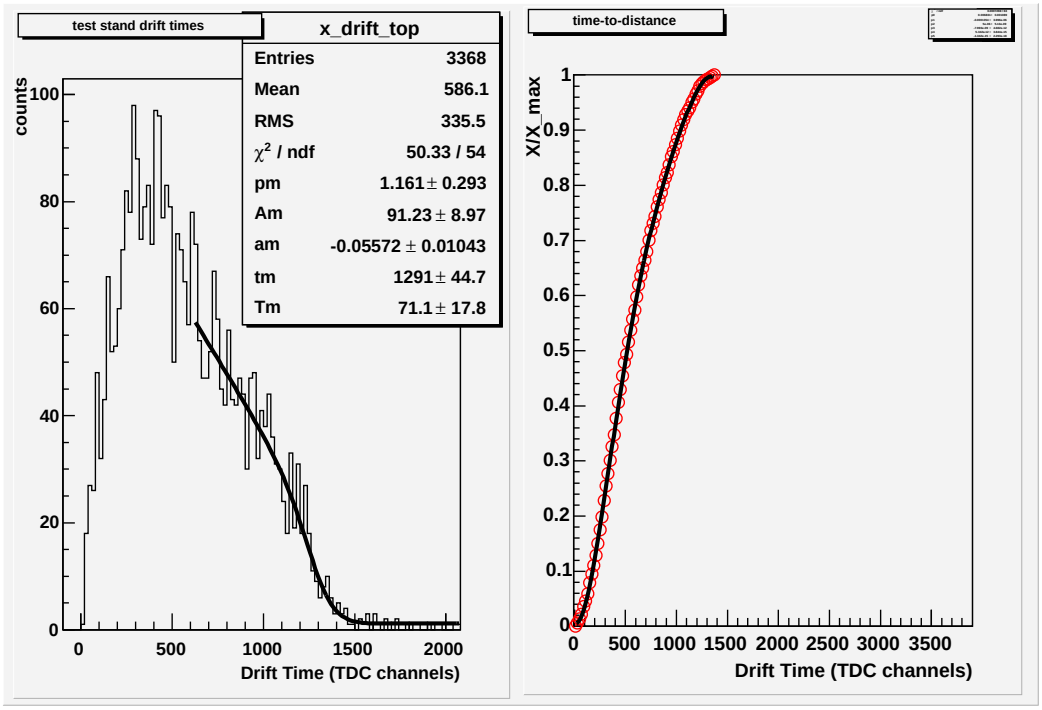


Figure 1: Sample drift time distribution and its integral for one of the test stand chambers. Each red circle on the right corresponds to the integral of left distribution from 0 to $t$ relative to the integral from 0 to $t_{max}$.

| Layer | $\sigma_x$ ($\mu$m) | $\sigma_y$ ($\mu$m) |
|---|---|---|
| 0 | 193 | 221 |
| 1 | 219 | 220 |
| 2 | 234 | 230 |
| 3 | 216 | 215 |

Table 1: Gaussian resolutions of the residual peaks for the x- and y-stacks after calibration.

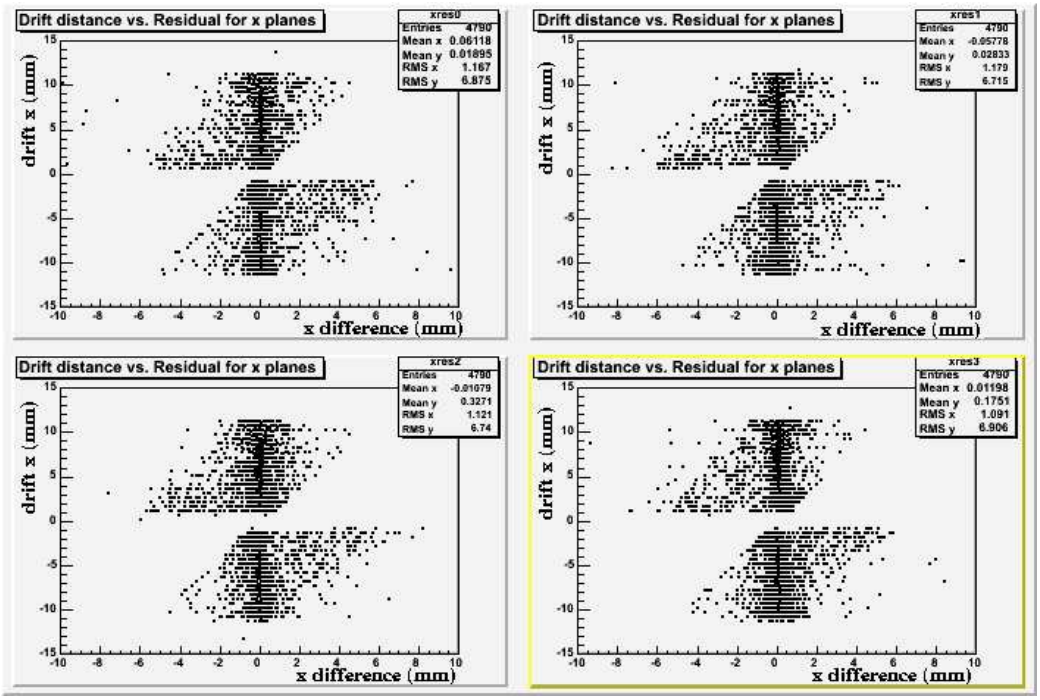


Figure 2: Drift distance verses track residuals for the four x-stack chambers.

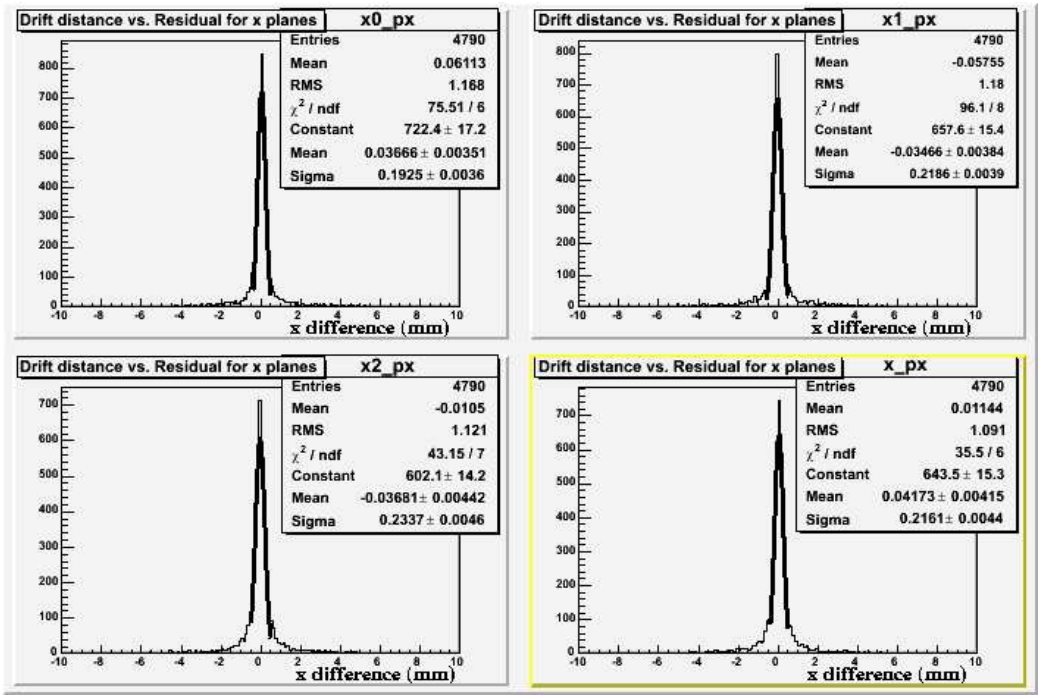


Figure 3: Track residuals for the four x-stack chambers with Gaussian fits superimposed.

| Peak position (mm) | Resolution ($\mu$m) |
|---|---|
| 270.1 | 154.0 |
| 280.2 | 169.5 |
| 290.2 | 158.1 |
| 300.1 | 178.6 |
| 310.2 | 165.1 |
| 320.2 | 177.9 |
| 330.2 | 162.2 |
| 340.2 | 175.6 |
| 350.2 | 174.7 |
| 360.2 | 187.4 |

Table 2: Quality of reconstruction of prototype wire positions using both cathode views.

is described in [1]. Since this earlier report we have been able to refine the functional representation of the strip charge distribution. We use a slightly modified version of the Mathieson/Gatti distribution used in [1]:

$$\frac{\rho(\lambda)}{q_a} = \frac{\pi k_2}{16}\left(1 - \tanh^2 \frac{\pi k_2 \lambda}{4}\right), \tag{3}$$

where $\lambda = x'/h$ is the ratio of the coordinate transverse to the strips relative to the "half-gap" (anode-cathode separation), $\rho(\lambda)$ is the induced charge distribution on a given strip plane, $q_a$ is the anode charge, and $k_2 \approx 1.15$ is an empirical constant. We use 5 adjacent strips in the centroid fits for the two cathode layers. Table 2 demonstrates how well we can now reconstruct the wire positions using this improved technique; the peaks we fitted to obtain the results for the table are shown in figure 4A.

In order to get a precise measurement of the distance away from the wire that the track passed through the prototype, we need to use the timing information from the wires. The anode signals are discriminated by CAMAC discriminators and the resulting pulses are digitized by F1 TDCs. Because the current configuration does not include field-shaping wires, the drift time distribution consists of a "prompt" timing peak plus a long tail to longer drift times, as shown in figure 4B. A figure from Sauli[3] (reproduced as figure 5 here) suggests how this timing distribution may be interpreted: the first peak in figure 4B seems to correspond to region A (ionization occurring near the

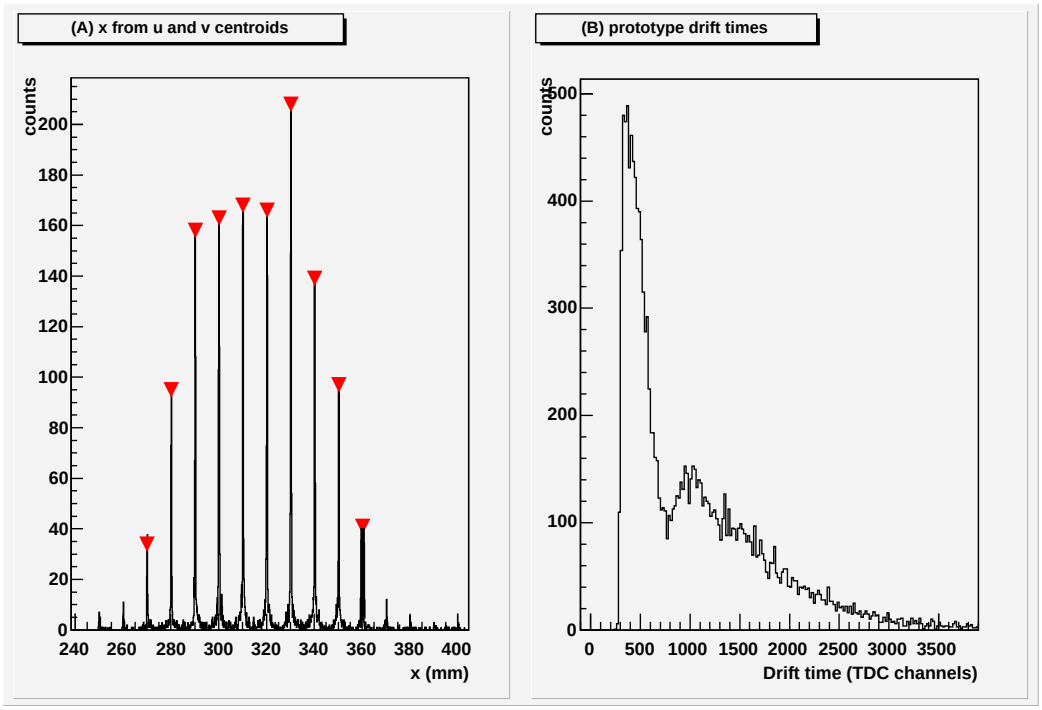


Figure 4: (A) Reconstruction of the prototype anode wire positions using only the cathode information; (B) Drift time distribution, summed over all the anode wires.

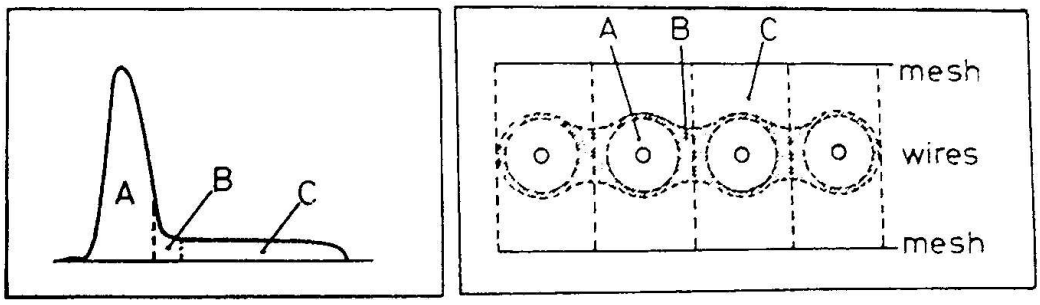


Figure 5: Cartoon of the timing properties of multi-wire proportional chambers, from Sauli[3].

wire) in figure 5. Consequently, to find the time-to-distance relation, we only take hits from the "prompt peak" with $t_0 = 200$ channels and $t_{max} = 800$ channels, which would correspond to the maximum drift distance $x_{cell} = 5$ mm. The same integration and fitting technique as was used for the test stand chambers was used to determine the prototype time-to-distance relationship.

Now we have enough information in both the x and y directions to compare the prototype measurements to the projections of the tracks to the plane of the prototype wires. These comparisons are shown in figure 6. The correlation plots both have slopes close to 1; however, the resolutions of the $\Delta x$ and $\Delta y$ distributions are on the order of 1 mm, which is not understood at the moment.

The current plan is to instrument the readout of the strips with Flash-ADCs. We have been considering the feasibility of instrumenting the wires with Flash-ADCs as well, for which the time would have to be extracted from the leading edges of the digitized pulses. We have added an 8-channel 105 MHz Struck Flash-ADC to the VME crate in the test stand electronics rack. Two wires (numbers 7 and 12) and 6 adjacent strips have been connected to the Flash-ADC. The lower-gain outputs of the VPI postamps were used for these signals, so the old CAEN ADC readout for these strips is still in place. Similarly the wires are still being discriminated with the CAMAC discriminators and the time registered by an F1TDC so that a direct comparison can be made. Figures 7 and 8 show the flash-ADC data from one of the wires and four strips for a sample event. The rise in area above the background underneath the pulses as the strip number decreases is readily apparent.

To extract the time we have fitted the rising edge of the pulse with a

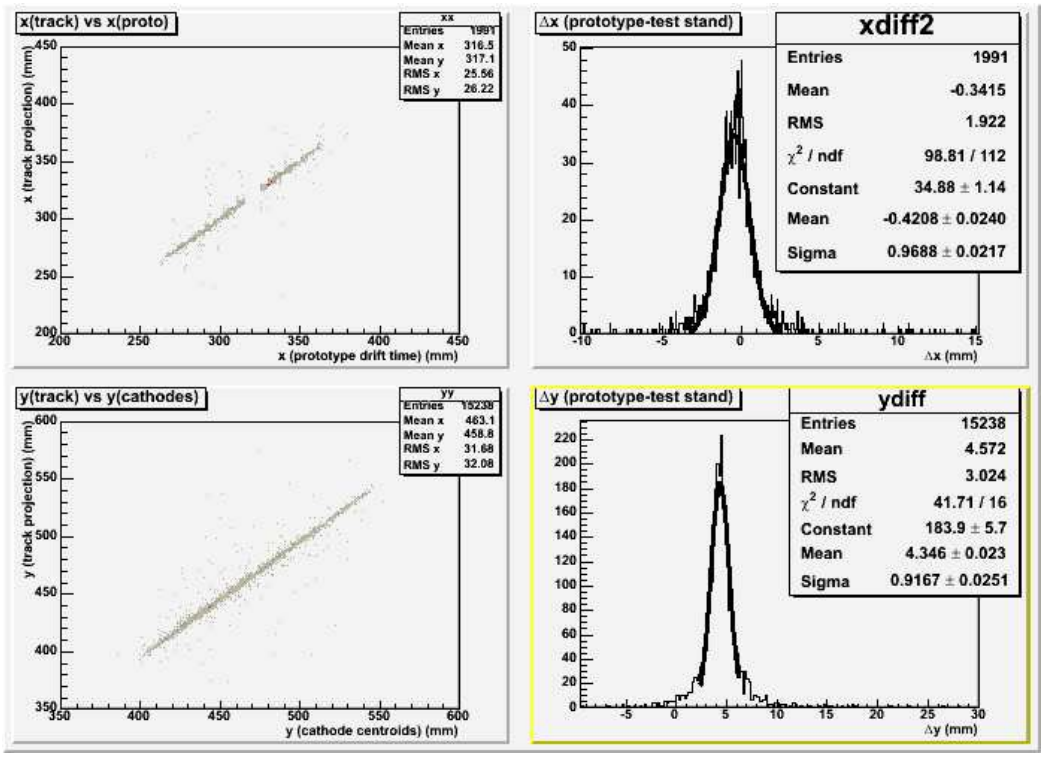


Figure 6: Correlation and difference plots between the track projected to the prototype plane and the positions in x and y extracted from the prototype data.

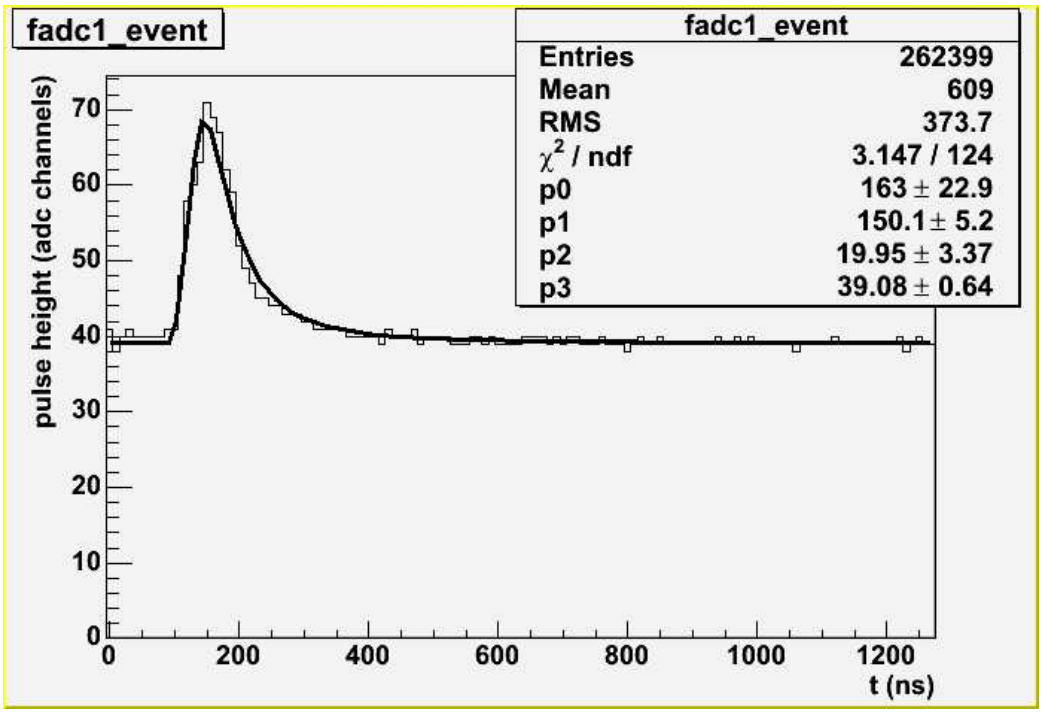


Figure 7: Flash-ADC data from an anode wire for a single muon event. The curve is the result of a fit using a Root Landau distribution and a flat background term.

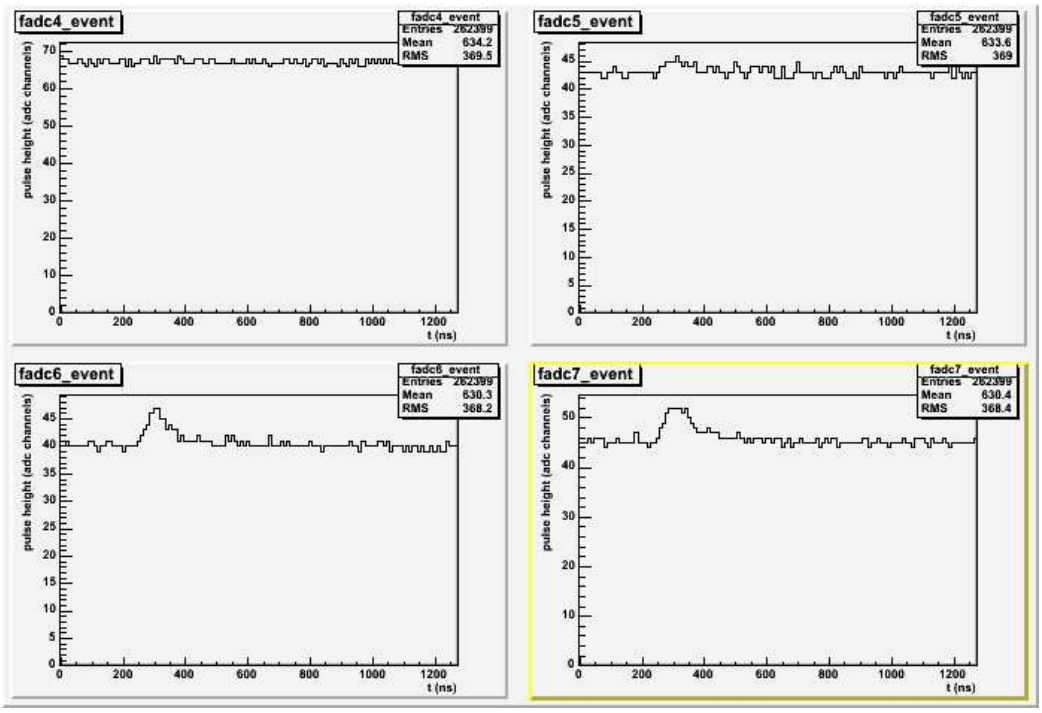


Figure 8: Flash-ADC data from 4 adjacent strips for the same event as figure 7.

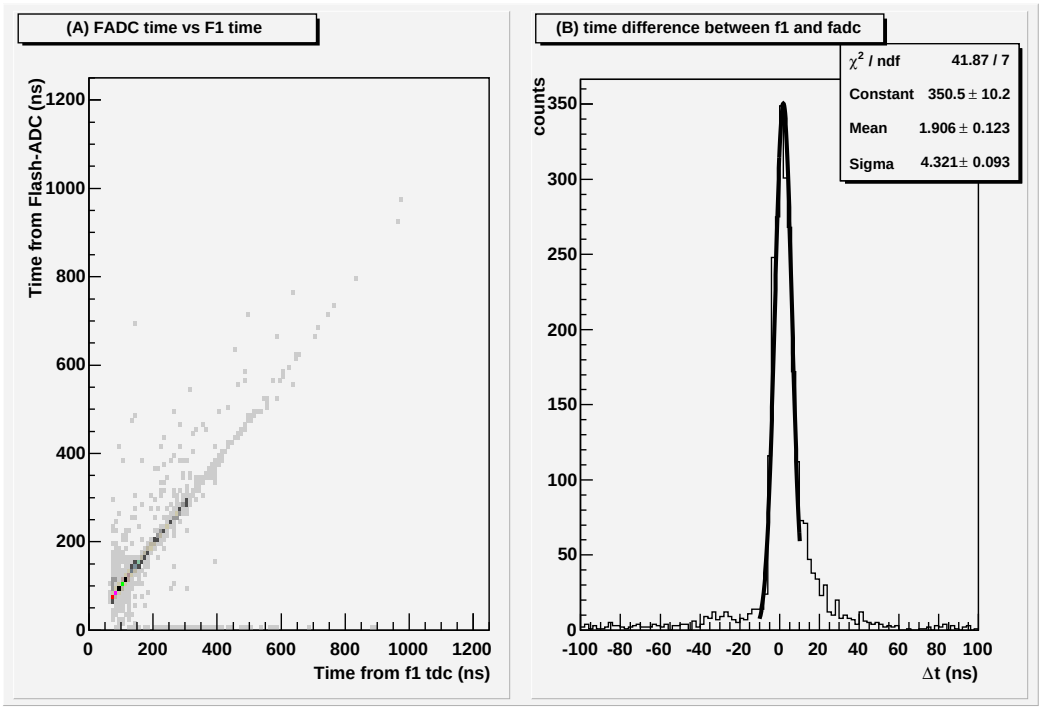


Figure 9: Correlation and difference between the times of hits from a single wire using two methods (extrapolation from the FADC data and using the discriminated output of the postamp).

line and finding the place at which the line crosses the background. Figure 9 compares the result from wire 12 using this method to the time obtained from discriminating the pulse from the postamp and digitizing the resulting logic signal with the F1 TDC. Generally these times are well-correlated but for smaller times there is a fair amount of poorly-correlated data. The resolution of the time difference gives some idea of how well the FADC timing method works, which at the moment is not very well.

# References

[1] S. Taylor and D. S. Carman, GlueX-doc-453-v1.

[2] O. Biebel, *et al.*, "A Cosmic Ray Measurement Facility for ATLAS Muon Chambers", LMU-ETP-2003-01, arXiv:physics/0307147.

[3] F. Sauli, "Principles of Operation of Multiwire Proportional and Drift Chambers", CERN 77-09.